Non-Isothermal Crystallization Kinetics as a Probe for Molecular Interactions in Biobased Semi-Aromatic Polyester. The Effect of Furan, Thiophene and Benzene Ring.

Matteo Venturi[a], Nadia Lotti[a,b,c], Michelina Soccio[a,b,d]* and Nicolas Sbirrazzuoli[e,]*

[a] Department of Civil, Chemical, Environmental and Materials Engineering, University of Bologna, Via Terracini 28, Bologna, 40131, Italy.

[b] Interdepartmental Center for Industrial Research on Advanced Applications in Mechanical Engineering and Materials Technology, CIRI-MAM, Viale del Risorgimento 2, 40136, Bologna, Italy.

[c] Interdepartmental Center for Industrial Agro-Food Research, CIRI-AGRO, Via Quinto Bucci 336, 47521, Cesena Italy.

[d] Interdepartmental Center for Industrial Research on Buildings and Construction CIRI-EC, Via del Lazzaretto 15/5, 40131, Bologna, Italy.

[e] Institut de Chimie de Nice, Université Côte d'Azur, CNRS, UMR 7272, 06108 Nice, France.

E-mail: m.soccio@unibo.it, Nicolas.SBIRRAZZUOLI@univ-cotedazur.fr

Monomer and polymer synthesis and characterization

2,5-Thiophenedicarboxylate dimethyl ester (DM-TFDC) was synthesized through esterification of TFDCA. Briefly, 15g of TFDCA were refluxed in 225 mL of methanol until complete dissolution occurred. After cooling to RT, 15.5 mL of thionyl chloride were added dropwise to the solution before refluxing for additional three hours. The solution was cooled in an ice bath to precipitate the product that was filtered and washed with cold methanol and DCM. ^{1}H-NMR (400Mz, dDMSO): δ = 7.82 (s, 2H), 3.86 (s, 6H).

PBF, PBTF, and PBI were synthesized via a previously optimized two-step melt polycondensation process starting from the corresponding dimethyl ester. A stoichiometric excess of 30% BD was used for PBF and PBI, while a 150% excess was employed for PBTF. Titanium (IV) butoxide (0.1 wt%) served as a catalyst. Reactions were carried out in a 250 mL glass reactor under mechanical stirring. In the first step, the mixture was heated to 180°C under a nitrogen atmosphere until about 80–90% of the theoretical methanol was distilled off. In the second step of the reaction, the mixture was heated to 210°C and the pressure was gradually reduced, using a mechanical vacuum pump, until reaching a constant value of 0.085 mbar. These conditions were maintained for approximately 3 hours, or until a constant torque was reached and no further BD was distilled anymore.

Purification of each polymer, through dissolution in chloroform, together with a few drops of HFIP for PBF and PBTF, followed by reprecipitation in methanol, was performed before further characterization.

The polymer structure was characterized via ^{1}H-NMR spectroscopy using a Agilent Varian Inova 400 MHz (Palo Alto, CA, USA) spectrometer. Samples were prepared dissolving 20 mg of the polymers in 0.7 mL of $CDCl_3$ adding a few drops of trifluoroacetic acid immediately before the analysis to facilitate the dissolution of PBF and PBTF. The molecular weight was assessed via intrinsic viscosity measurements in a 60:40 PhOH-TCE mixture.

^1H-NMR (400 MHz, $CDCl_3$). PBF: δ = 7.26 (s, 2H), 4.42 (t, J = 5.5 Hz, 4H), 1.92 (m, 4H) – PBTF: δ = 7.78 (s, 2H), 4.44 (m, 2H), 1.95 (m, 2H) – PBI: δ = 8.64 (t, J = 1.8 Hz, 1H), 8.19 (dd, J = 7.8, 1.7 Hz, 2H), 7.49 (t, J = 7.8 Hz, 1H), 4.41 (d, J = 5.3 Hz, 4H), 1.94 (m, 4H).

IV: PBF 1.03 ± 0.03 dL g^{-1} – PBTF 0.96 ± 0.01 dL g^{-1} – PBI 0.80 ± 0.03 dL g^{-1}.

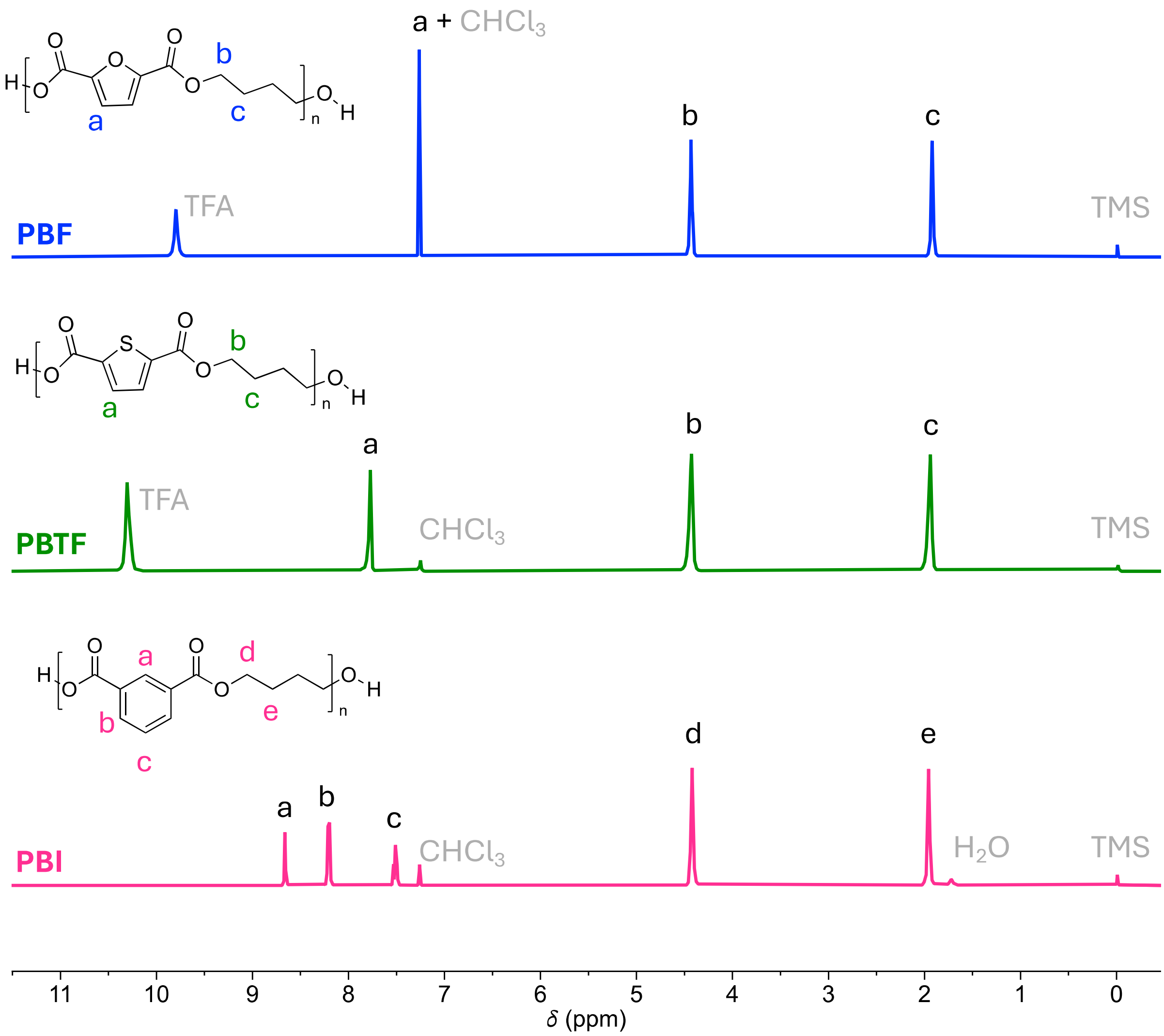

Figure S1. 400Mz ^{1}H-NMR spectra of PBF (blue), PBTF (green) and PBI (pink) in $CDCl_3$.

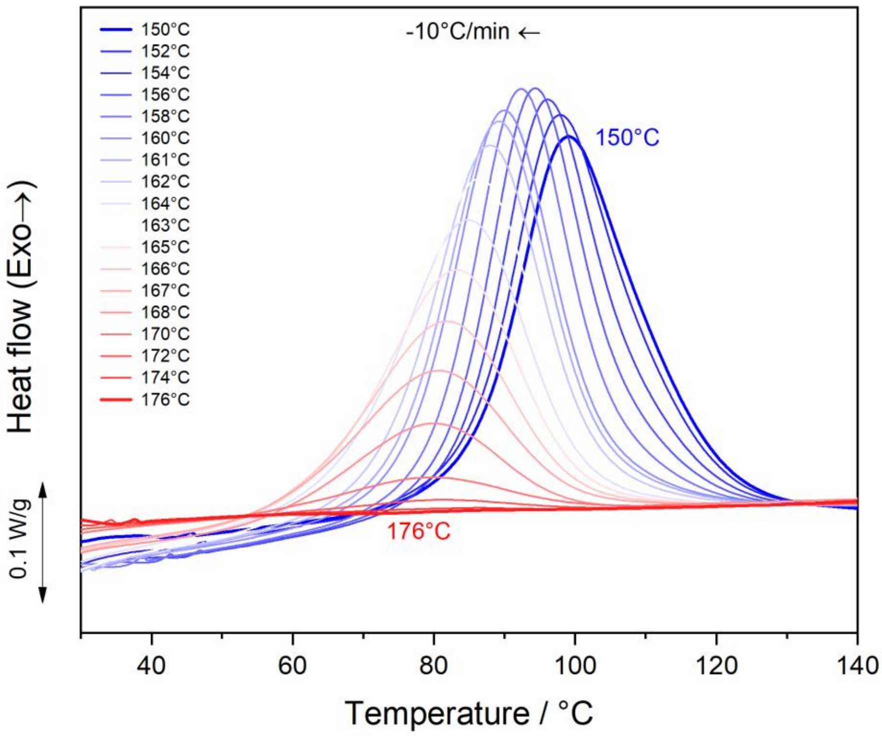

Figure S2. Evolution of the crystallization peak of PBI under a cooling ramp of -10°C/min as the melt is equilibrated at progressively higher temperatures before cooling.

Table S1. Thermodynamic data for crystallization from the glass

Rate	T_g (°C)	ΔC_p (J/°Cg)	T_c (°C)	ΔH_{cc} (J/g)	$T_{m,1}$ (°C)	$T_{m,2}$ (°C)	ΔH_m (J/g)
				PBF			
1°C/min	35.4	0.331	75.2	35.1	-	172.8	37.2
2°C/min	35.5	0.450	80.9	37.9	-	171.5	38.4
5°C/min	37.1	0.469	91.3	39.3	-	169.7	38.8
7°C/min	37.7	0.466	96.0	41.2	-	169.3	37.6
10°C/min	38.2	0.481	101.9	41.1	-	168.3	38.3
				PBTF			
1°C/min	21.8	0.501	59.9	31.0	-	154.8	34.7
2°C/min	23.8	0.451	64.9	30.0	-	153.6	31.2
5°C/min	25.2	0.435	73.1	32.0	-	151.6	32.4
7°C/min	24.8	0.474	76.8	33.0	-	151.0	32.3
10°C/min	25.8	0.409	81.9	28.4	-	150.7	29.6
				PBI			
1°C/min	22.0	0.494	68.6	39.2	-	148.1	46.3
2°C/min	18.9	0.480	74.8	41.6	-	146.3	41.6
5°C/min	23.6	0.462	86.2	42.0	129.6	144.4	42.1
7°C/min	25.1	0.408	92.1	42.7	133.7	143.9	40.0
10°C/min	26.0	0.412	91.1	37.2	133.2	142.9	34.7

Table S2. Thermodynamic data for crystallization from the melt

Rate	T_g (°C)*	ΔC_p (J/°Cg)	T_c (°C)	ΔH_c (J/g)	$T_{m,1}$ (°C)	$T_{m,2}$ (°C)	ΔH_m (J/g)*
			PBF				
-1°C/min	40.4	0.186	140.4	41.5	122.67	169.9	38.2
-2°C/min	41.4	0.141	135.4	44.1	127.32	169.6	39.8
-5°C/min	40.2	0.152	126.1	43.0	132.21	169.3	42.4
-7°C/min	40.4	0.092	122.2	42.5	142.45	169.1	34.8
-10°C/min	42.7	0.151	117.3	41.6	148.1	168.9	46.8
			PBTF				
-1°C/min	28.9	0.165	113.4	33.5	-	149.7	38.7
-2°C/min	28.6	0.149	106.2	32.8	-	150.4	35.5
-5°C/min	28.1	0.138	94.7	31.9	-	151.7	28.1
-7°C/min	28.3	0.145	89.1	31.4	-	151.6	27.4
-10°C/min	27.3	0.152	84.8	27.0	-	151.2	30.0
			PBI				
-1°C/min	26.4	0.241	116.5	38.2	-	141.0	37.8
-2°C/min	25.7	0.210	110.4	42.7	-	139.6	38.4
-5°C/min	25.5	0.210	99.1	40.0	-	140.0	40.1
-7°C/min	25.9	0.223	93.4	36.8	-	141.0	48.1
-10°C/min	24.9	0.227	86.3	32.5	-	141.5	41.4

*Value extracted from heating scan at 10°C/min subsequent to the crystallization cooling ramp

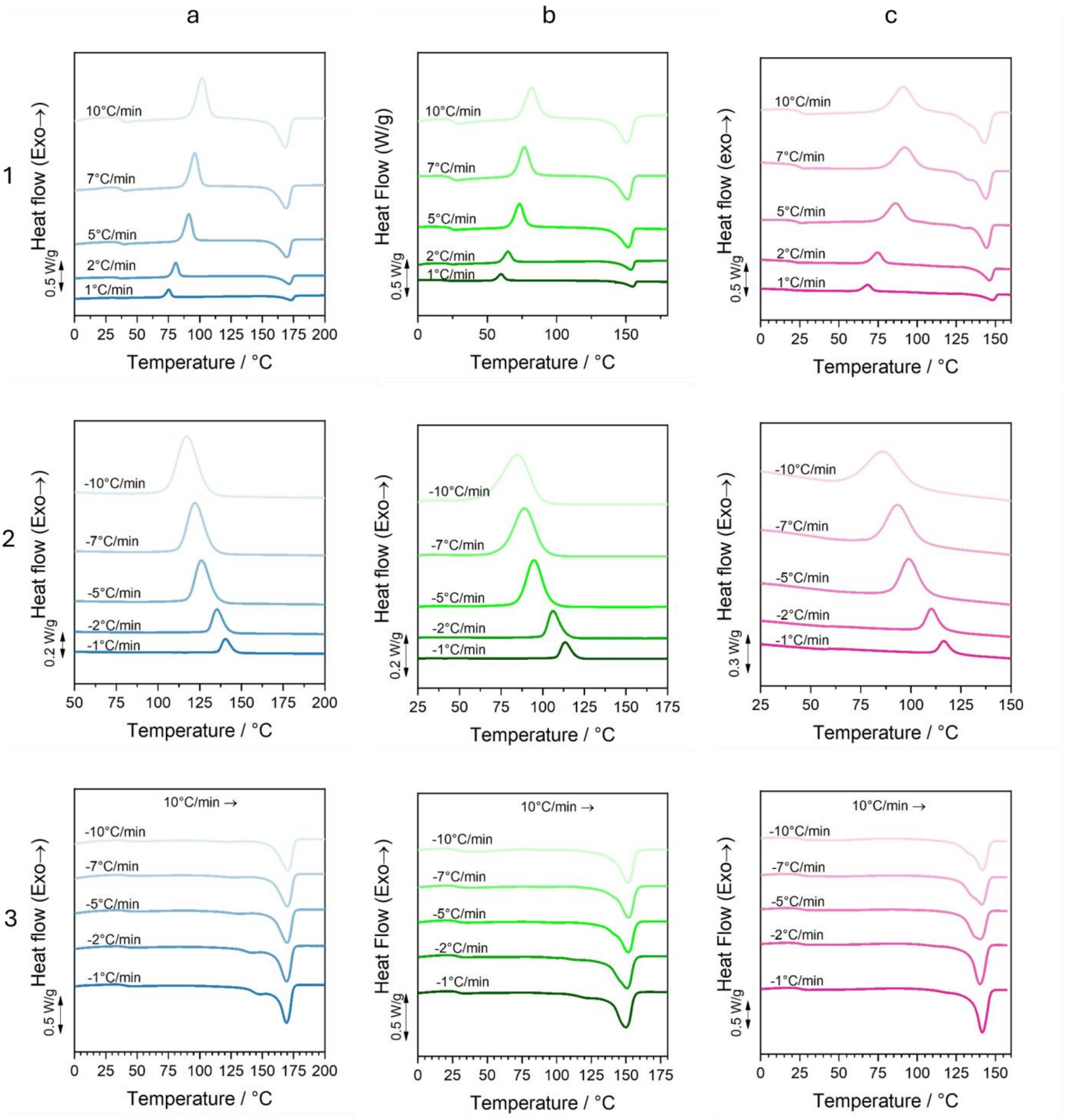

Figure S3. DSC curves relative to the non-isothermal crystallization experiments. On the first line crystallization from the glass, on the second line (2) crystallization from the melt and on the third line melting after crystallization from the melt at different cooling rates revealed at 10°C/min for the different polymers. Each polymer is represented in a different column: PBF (a), PBTF (b) and PBI (c).

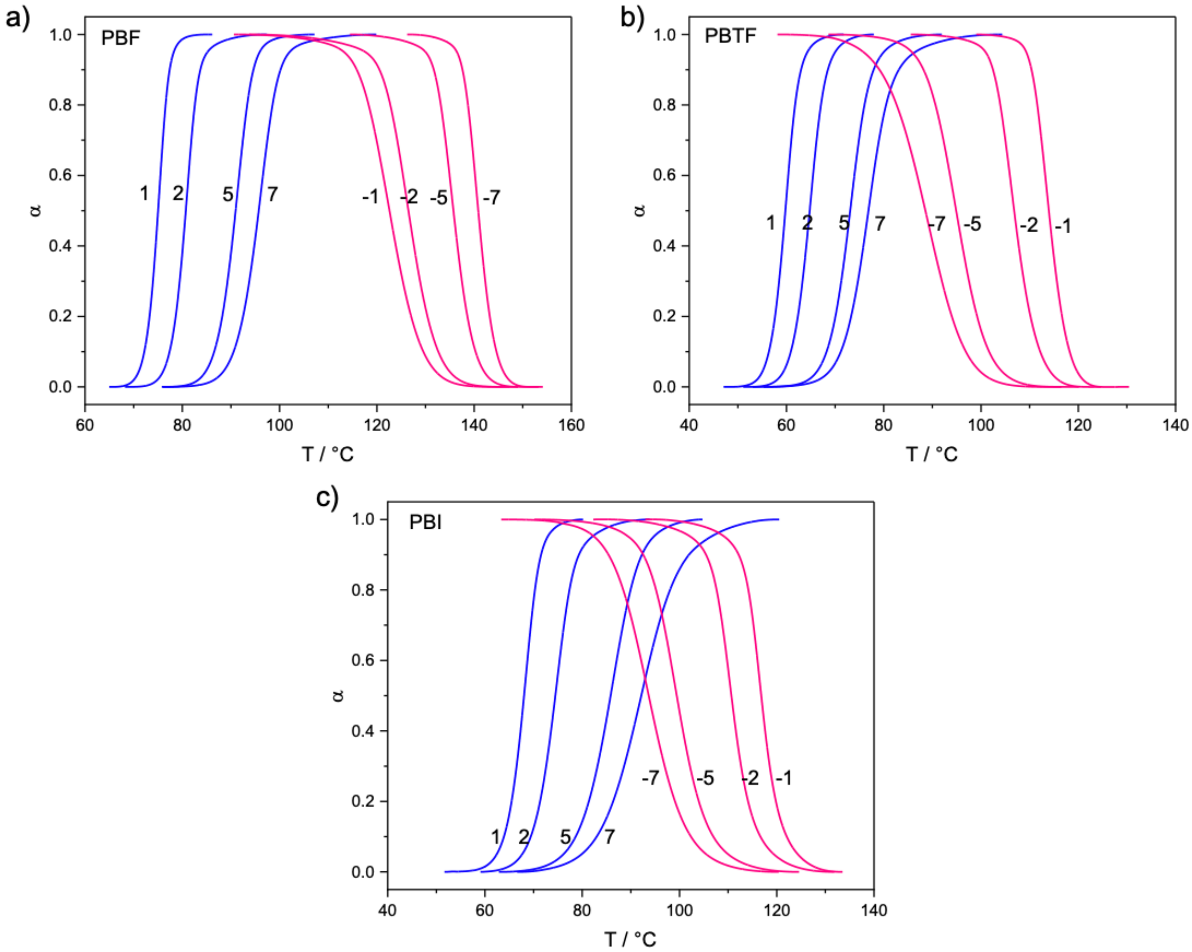

Figure S4. Relative extent of crystallization (α) on heating and on cooling vs temperature (T) of PBF (a), PBTF (b) and PBI (c). The heating/cooling rates in °C/min are indicated by the curves.

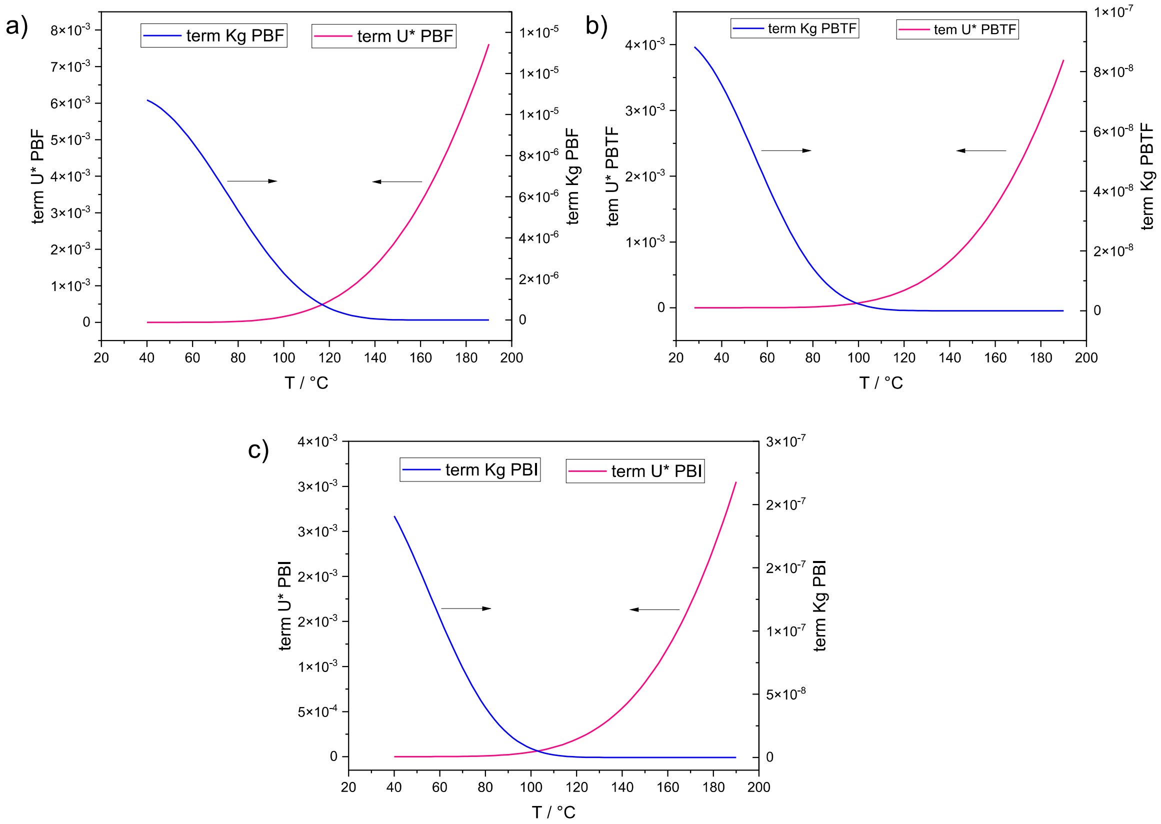

Figure S5. Dependence of the terms U^* and K_g for PBF (a), PBTF (b) and PBI (c).

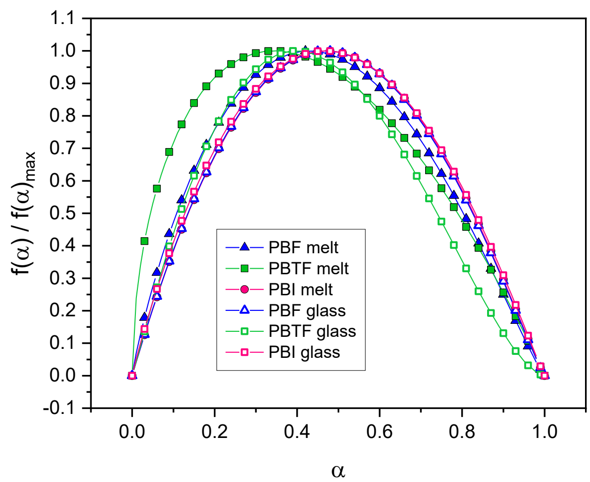

Figure S6. Variation of the normalized function $f(\alpha) = \alpha^m (1- \alpha)^n$ with α using the computed values of the kinetic exponents m and n for PBF, PBTF and PBI reported in Tables 3-5.

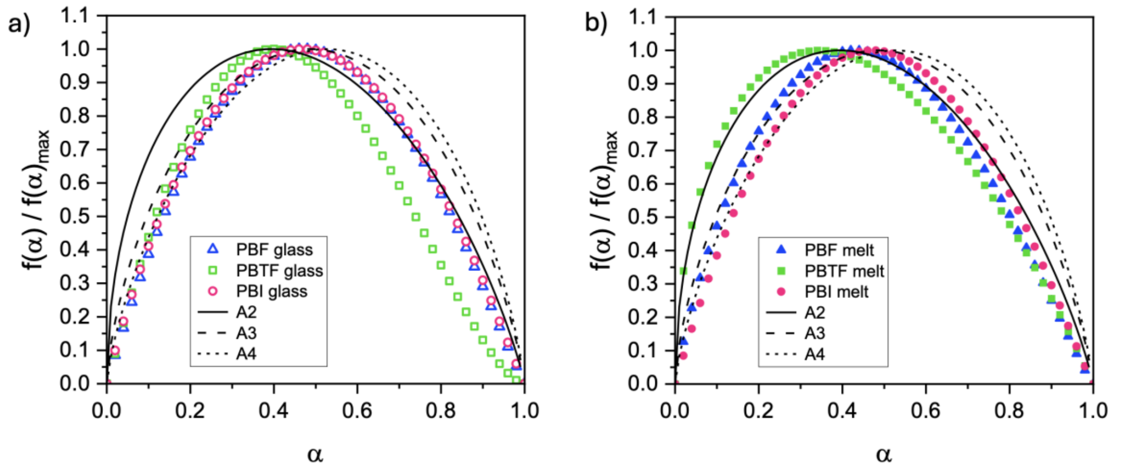

Figure S7. Comparison of the variation of the normalized function $f(\alpha) = \alpha^m (1- \alpha)^n$ for the investigated polymers upon crystallization from the glass (a) and from the melt (b), with the functions associated to the mechanism A2, A3, and A4 of JMAEK's model.